

The Power Spectrum of Cosmological Number Densities

Amanda R. Lopes,^{1*} Marcelo B. Ribeiro^{2**} and William R. Stoeger^{3***}

¹ Valongo Observatory, Universidade Federal do Rio de Janeiro, Rio de Janeiro, Brazil

² Physics Institute, Universidade Federal do Rio de Janeiro, Rio de Janeiro, Brazil

³ Vatican Observatory Research Group, Steward Observatory, University of Arizona, Tucson, USA

ABSTRACT

Aims. This paper studies the cosmological power spectrum (PS) of the differential and integral galaxy volume number densities, respectively γ_i and γ_i^* , constructed with the cosmological distances d_i ($i = A, G, L, Z$), where d_A is the angular diameter distance, d_G is the galaxy area distance, d_L is the luminosity distance and d_z is the redshift distance. Theoretical and observational quantities were obtained in the Friedmann-Lemaître-Robertson-Walker (FLRW) spacetime with a non-vanishing cosmological constant. The radial correlation Ξ_i , a quantity defined in the context of these densities, is also discussed in the wave number domain. All observational quantities were computed using luminosity function (LF) data obtained from the FORS Deep Field (FDF) galaxy survey.

Methods. The theoretical and observational power spectra of γ_i , γ_i^* , Ξ_i and the ratio γ_i/γ_i^* were calculated by performing Fourier transforms on values of these densities which were previously derived by Iribarrem et al. (2012) from the observational values $[\gamma]_{\text{obs}}$ and $[\gamma^*]_{\text{obs}}$ obtained by using the galactic absolute magnitudes and Schechter's parameters of the galaxy LF presented in Gabasch et al. (2004, 2006). These parameters were evaluated from a I-band selected dataset of the FDF in the redshift range $0.5 \leq z \leq 5.0$ for its blue bands and $0.75 \leq z \leq 3.0$ for its red ones.

Results. The results show similar behavior of the power spectra obtained from γ and γ^* using d_L , d_z and d_G as distance measures. The PS of the densities defined with d_A have a different and inconclusive behavior, as this cosmological distance reaches a maximum at $z \approx 1.6$ in the adopted cosmological model. For the other distances, our results suggest that the PS of $[\gamma_i]_{\text{obs}}$, $[\gamma_i^*]_{\text{obs}}$ and $[\gamma_i/\gamma_i^*]_{\text{obs}}$ have a general behavior approximately similar to the power spectra obtained with the galaxy two-point correlation function and, by being sample size independent, they may be considered as alternative analytical tools to study the galaxy distribution.

Key words. galaxies: power spectrum – galaxies: number densities – galaxies: distances and redshifts – large-scale structure of Universe

1. Introduction

The *galaxy volume number densities* are important measures in cosmology as they give information about the evolving universe mass-energy content and allow us to test cosmological models. This is so because they are able to connect theory and observation once different types of number densities are evaluated, both theoretically and observationally. Theoretically, these densities can be obtained once one chooses a cosmological spacetime geometry, usually the standard model given by the spatially homogeneous Friedmann-Lemaître-Robertson-Walker (FLRW) cosmology or, in a recent trend, the spatially inhomogeneous Lemaître-Tolman-Bondi cosmology as well (Iribarrem et al. 2013, 2014). Observationally, inasmuch as the galaxy *luminosity function* (LF) is a number density per unit luminosity, several authors have been systematically determining galaxy volume number densities using the LF derived from galaxy redshift surveys.

Comparing cosmological models with observations using number densities determined from LF parameters derived from observed data requires, however, some model connecting relativistic cosmology number counts theory to the LF astronomical data and practice. One way of pursuing this theoretical link was advanced by Ribeiro & Stoeger (2003, hereafter RS03) who used general relativistic theory to obtain specialized expressions ca-

pable of being applied to LF data. Albani et al. (2007, hereafter A07) and Iribarrem et al. (2012, hereafter Ir12) further extended such a link and applied the connecting expressions to the data of the Second Canadian Network for Observational Cosmology (CNOC2; see Lin et al. 1999) and FORS Deep Field (FDF; see Gabasch et al. 2004, 2006; hereafter G04 and G06 respectively) galaxy redshift surveys. Following the methodology advanced by Ribeiro (2005; see also Rangel Lemos & Ribeiro 2008) for number density definitions, where the adoption of cosmological distance measures is made explicit, A07 and Ir12 calculated the *differential number density* γ and its *integral* counterpart γ^* for various cosmological distances and used them to study the observational inhomogeneities in the relativistic radial distribution of galaxies (Ribeiro 2001) belonging to both datasets in the FLRW universe model. Their results indicated that observational inhomogeneities in the relativistic galaxy distribution can arise due to geometrical, past-light cone, effects even in the context of spatially homogeneous cosmologies.

Analyzes of the large-scale structure of the universe use, however, a complementary tool to examine such structures, the *power spectrum* (PS), which is basically a Fourier transform of the quantity under study. If galaxies form the basic units of a cosmological fluid described by a volume number density, this galactic fluid can also be considered as being composed of wave densities with different wave numbers. Then, the PS will give us the intensity, or power, in each component. This is essentially the PS analysis of the galaxy 2-point correlation function, as the information given by the PS is complementary to the correlation function. Various authors performed such an analysis (e.g. Sylos

* amandalopes1920@gmail.com

** mbr@if.ufrj.br

*** In memoriam (1943-2014)

Labini et al. 1998; Martínez & Saar 2002; Tegmark et al. 2004, 2006; Gabrielli et al. 2005) and showed that, in general, the PS behavior is a power-law. Since galaxy volume number densities were used by RS03, A07 and Ir12 to analyze the universe matter-energy content and evolution, it is natural to expand these studies to include a PS analysis.

The goal of this work is to study the differential and integral number densities γ and γ^* in the wave number domain through the PS. This is achieved by performing Fourier transforms of both quantities. Using the relativistic analysis and results presented by Ir12, we computed the theoretical power spectra of γ_i and γ_i^* obtained using the cosmological distance d_i . Here the index i stands for the adopted distance measure, namely the *angular diameter distance* d_A , also known as *area distance*, *galaxy area distance* d_G , *luminosity distance* d_L and *redshift distance* d_z ($i = A, G, L, z$). Observational values of the differential and integral densities computed with these distance measures, $[\gamma_i]_{\text{obs}}$ and $[\gamma_i^*]_{\text{obs}}$, were obtained using the results of Ir12, which employed the LF parameters derived by G04 and G06 from the FDF survey data. The analysis is also extended to include the power spectra of the *ratio* γ/γ^* and of another quantity, named here as *radial correlation* Ξ , which is basically a radial function whose behavior in terms of d_i bears some similarities to the 2-point correlation function (Ribeiro 1995).

The distance measures $d_i(z)$ were obtained in the cosmology adopted here: the FLRW model with non zero cosmological constant Λ and parameter values equal to $\Omega_{m_0} = 0.3$, $\Omega_{\Lambda_0} = 0.7$ and $H_0 = 70 \text{ km s}^{-1} \text{ Mpc}^{-1}$. The dataset studied here is the I-band selected luminosity functions of the FDF survey. Ir12 calculated observed differential number counts and then $[\gamma_i(z)]_{\text{obs}}$ and $[\gamma_i^*(z)]_{\text{obs}}$ using the absolute magnitudes, LF Schechter parameters and their respective redshift parametrization, all previously derived by G04 and G06 directly from the FDF data in eight bandwidths with a redshift range $0.5 \leq z \leq 5.0$, for the blue bands (G04), and $0.45 \leq z \leq 3.75$ for the red bands (G06). Those results allowed us to calculate the ratio $[\gamma_i/\gamma_i^*]_{\text{obs}}$ and the radial correlation $[\Xi_i(d_i)]_{\text{obs}}$. Fourier transforms on these quantities provided their respective power spectra, $P_k[\gamma_i]_{\text{obs}}$, $P_k[\gamma_i^*]_{\text{obs}}$, $P_k[\gamma_i/\gamma_i^*]_{\text{obs}}$ and $P_k[\Xi_i]_{\text{obs}}$.

The results show that power spectra analyzes with the angular diameter distance d_A is problematic, because each d_A corresponds to two different values for z , since this distance starts from zero, grows to maximum and then tends to zero as $z \rightarrow \infty$. This maximum d_A value is the only one with unique redshift. Due to these features the results obtained with d_A turn out to be problematic in terms of interpretation.

We were also able to reproduce the preliminary results of Ribeiro (1995) regarding the radial correlation, confirming its dependency with the sample size and finding out that its respective PS is also sample size dependent. The best results, however, were obtained with the power spectra of the differential and integral densities using d_L and d_z , which show a behavior bearing similarities, even at wave number values, with the 2-point correlation function PS. This suggests that PS analysis of number densities can also be a complementary tool for large-scale structure studies.

The plan of the paper is as follows. In §2 the basic quantities used in this paper are presented, as well as the expressions required in their calculation. §3 specializes the previously discussed general quantities to the FLRW cosmological model and shows how the luminosity function parameters of the FDF survey are used to calculate the desired observational expressions. §4 presents both the theoretical and observation results of all

quantities discussed here, as well as their respective power spectra, and §5 presents our conclusions.

2. Basic Definitions

This section defines the basic quantities and expressions necessary for the PS analysis discussed here. Although they have already been introduced in previous papers (Ribeiro 1995, 2005; Rangel Lemos & Ribeiro 2008; A07; Ir12), one can find below a few additional clarifying remarks.

2.1. Differential and Integral Densities

Let us start by defining the two key quantities used in this study. The *differential density* γ_i gives the rate of growth in number counts, or more precisely in their density, as one moves along the observational distance d_i . It is defined by the following expression (Ribeiro 2005),

$$\gamma_i = \frac{1}{4\pi(d_i)^2} \frac{dN}{d(d_i)}, \quad (1)$$

where N is the *cumulative number counts*. The *integrated differential density*, or simply *integral density*, γ_i^* gives the number of sources per unit of observational volume located inside the observer's past light cone down to a distance d_i . It is written as follows,

$$\gamma_i^* = \frac{1}{V_i} \int_{V_i} \gamma_i dV_i, \quad (2)$$

where V_i is the *observational volume*,

$$V_i = \frac{4}{3}\pi(d_i)^3. \quad (3)$$

As it has been previously discussed, these quantities are useful in determining whether or not, and at what ranges, a spatially homogeneous cosmological model exhibits observational inhomogeneity because these densities behave very differently depending on the distance measure used in their definitions. In other words, they show a clear dependence on the adopted cosmological distance (Ribeiro 2005; Rangel Lemos & Ribeiro 2008; A07; Ir12).

It is useful to write the two number densities above in terms of the redshift. Thus, the differential density (1) may be written as,

$$\gamma_i = \frac{dN}{dz} \left\{ 4\pi(d_i)^2 \frac{d(d_i)}{dz} \right\}^{-1}, \quad (4)$$

where dN/dz is the *differential number counts*. In addition, the expressions above allow us to conclude that the following expression holds,

$$\gamma_i^* = \frac{N}{V_i}. \quad (5)$$

2.2. Radial Correlation

Studies of the large-scale galaxy structure have traditionally employed the 2-point correlation function as a tool to characterize the galaxy distribution, including the possible depth at which this distribution reached homogeneity. This latter application was, however, criticized by Pietronero (1987) who argued that

the correlation function actually presupposes homogeneity and, therefore, it is a tool unsuited to find its possible presence in the galaxy structure. In order to remove such a built-in hypothesis, Pietronero (1987) proposed a different correlation methodology by advancing the conditional density $\Gamma(d)$, where d is the distance, as the proper tool capable of detecting the possible homogeneity in the galaxy distribution. He also showed that Γ has a simple functional relationship to the 2-point correlation function ξ , given by the following expression (see also Sylos Labini et al. 1998; Gabrielli et al. 2005),

$$\xi(d) = \frac{\Gamma(d)}{\bar{n}(R)} - 1, \quad (6)$$

where $\bar{n}(R)$ is the mean density of the sample whose radius R defines the sample volume. This equation shows explicitly the correlation function dependence to the sample depth given by R .

Ribeiro (1995) followed these ideas and defined a radial quantity exhibiting the same sample dependence property, dubbed here as *radial correlation* Ξ . In the present context this quantity may be written as follows,

$$\Xi_i(d_i) = \frac{\gamma_i(d_i)}{\gamma_i^*(R_i)} - 1. \quad (7)$$

As the expressions above shows, Ξ is not a proper statistical correlation, but simply a dimensionless radial function that can be used in the context of number density distributions originated from relativistic cosmology theory, and whose behavior is also dependent on the sample depth, defined here at the radial distance $d_i = R_i$. Ribeiro (1995) studied this quantity in the context of the Einstein-de Sitter model using its theoretical distribution obtained in terms of the luminosity distance and redshift. Here, however, we shall employ the FLRW cosmology as well as the other distance measures discussed above in order to derive observational values for Ξ_i using the FDF galaxy survey.

2.3. Power Spectrum

If one assumes spherical symmetry, the PS of the 2-point correlation function is given by,

$$P_k(\xi) = 4\pi \int_0^\infty \frac{\sin(kx)}{kx} \xi(x) x^2 dx. \quad (8)$$

This function describes clustering in terms of the wave numbers k and separates the clustering effects in different scales. To study the differential densities in the wave number domain, we shall employ a similar definition as above, which may be written as follows,

$$P_k(\gamma_i) = \int_0^\infty \frac{\sin(kx)}{kx} \gamma_i(x) x^2 dx. \quad (9)$$

For astronomical observations contained in galaxy survey samples one needs, however, to consider the finiteness of the sample size and divide it in redshift bins so that the function above can actually be plotted from real data. This means rewriting the equation above as follows,

$$P_k[\gamma_i]_{\text{obs}} = \int_0^{d_i(z_j)} \frac{\sin(k_j d_i)}{k_j d_i} \gamma_i d_i^2 d(d_i). \quad (10)$$

Here $d_i(z)$ is the distance-redshift relation given by the adopted cosmological model in a certain distance measure,

$$k_j \equiv \frac{2\pi}{d_i(z_j)}, \quad \text{for } (j = 1, \dots, m), \quad (11)$$

where m is the total number of redshift bins dividing the sample and z_j is the central redshift value of j -th bin. Replacing γ_i with its definition given in Eq. (1) leads to the following expression,

$$P_k[\gamma_i]_{\text{obs}} = \frac{1}{4\pi} \int_0^{d_i(z_j)} \frac{\sin(k_j d_i)}{k_j d_i} \frac{dN}{d(d_i)} d(d_i). \quad (12)$$

Similarly, The PS of the integral densities yields,

$$P_k[\gamma_i^*]_{\text{obs}} = \int_0^{d_i(z_j)} \frac{\sin(k_j d_i)}{k_j d_i} \gamma_i^* d_i^2 d(d_i), \quad (13)$$

or, using Eqs. (3) and (5), it can also be written as,

$$P_k[\gamma_i^*]_{\text{obs}} = \frac{3}{4\pi} \int_0^{d_i(z_j)} \frac{\sin(k_j d_i)}{k_j d_i^2} N d(d_i). \quad (14)$$

3. Cosmologic and Sample Specific Expressions

The quantities defined above are general, that is, valid for any cosmological model. In this section we shall adopt the FLRW cosmology and calculate them in this specific universe model, as well as using galaxy redshift survey observations.

As a simple examination of the equations above shows, we only require cosmologic specific expressions for $d_i(z)$, $d(d_i)/dz$, $N(z)$, dN/dz , $[N]_{\text{obs}}$ and $[dN(z)/dz]_{\text{obs}}$. The first four quantities are theoretical and come from the chosen spacetime geometry, whereas the last two ones come from a combination of theoretical and observational results, as we shall see next.

3.1. FLRW Cosmological Model

In this cosmology we need to obtain the required quantities along the past null cone, a task that is carried out numerically. As Ir12 discusses such a procedure in great details, what we shall present next is just a summary of the results needed here.

The scale factor of the FLRW cosmology with non zero cosmological constant Λ can be written in terms of the radial coordinate r as follows,

$$\frac{dS}{dr} = -H_0 \left[\frac{(\Omega_{\Lambda_0})S^4 - S_0^2(\Omega_0 - 1)S^2 + (\Omega_{m_0}S_0^3)S}{c^2 - H_0^2 S_0^2 (\Omega_0 - 1)r^2} \right]^{\frac{1}{2}}, \quad (15)$$

where Ω_{m_0} and Ω_{Λ_0} are, respectively, the matter and cosmological density parameters, H_0 is the Hubble constant, S_0 is the current value of the scale factor, assumed to be equal to unity, and

$$\Omega_0 \equiv \Omega_{m_0} + \Omega_{\Lambda_0}. \quad (16)$$

To find solutions for $S(r)$ we shall use the following numerical values for the parameters above: $\Omega_{m_0} = 0.3$, $\Omega_{\Lambda_0} = 0.7$ and $H_0 = 70 \text{ km s}^{-1} \text{ Mpc}^{-1}$. The redshift z can be written as

$$1 + z = \frac{S_0}{S}, \quad (17)$$

where it is clear that a numerical solution of the scale factor also produces numerical solutions for $z(r)$. The differential number counts yields,

$$\frac{dN}{dz} = \left(\frac{3 c \Omega_{m_0} H_0 S_0^2}{2 G M_g} \right) \times \left[\frac{r^2 S^2}{\sqrt{(\Omega_{\Lambda_0})S^4 - S_0^2(\Omega_0 - 1)S^2 + (\Omega_{m_0}S_0^3)S}} \right], \quad (18)$$

where G is the gravitational constant, c is the light speed and \mathcal{M}_g is the average galactic rest mass, dark matter included.

As pointed out by A07 and Ir12, the details of the galaxy mass function and how it evolves with the redshift are imprinted in the LF itself and will be included in any observationally derived functions stemming from the LF. For the theoretical quantities, we shall assume a constant average galaxy rest mass with the working value of $\mathcal{M}_g \approx 10^{11} M_\odot$ based on the estimate by Sparke & Gallagher (2000). To actually extract from the LF the implicit galaxy mass function so that the function $\mathcal{M}_g(z)$ can be estimated and used in the theoretical quantities is a problem which we shall deal with in a forthcoming paper (Lopes et al. 2014, in preparation).

The angular diameter distance d_A is obtained by means of a relation between the intrinsically measured cross-sectional area element $d\sigma$ of the source and the observed solid angle $d\Omega_0$. In a spherically symmetric spacetime it may be written as follows (Ellis 1971, 2007; Ribeiro 2005; Plebański & Krasinski 2006),

$$(d_A)^2 = \frac{d\sigma}{d\Omega_0} = (Sr)^2. \quad (19)$$

The redshift distance is defined by the following expression,

$$d_z = \frac{cz}{H_0}, \quad (20)$$

and the remaining distance measures can be obtained from the area distance by means of the Etherington (1933) reciprocity law (Ellis 1971, 2007),

$$d_L = (1+z)^2 d_A = (1+z) d_G. \quad (21)$$

The particular case of this law relating only d_L to d_A is known as the distance duality relation and can be determined observationally (Holanda et al. 2010, 2011, 2012). Thus, considering Eqs. (17), (19) and (21) the other cosmological distances are straightforwardly written in terms of the scale factor as follows,

$$d_L = S_0^2 \left(\frac{r}{S} \right), \quad (22)$$

$$d_G = S_0 r, \quad (23)$$

$$d_z = \frac{c}{H_0} \left(\frac{S_0}{S} - 1 \right). \quad (24)$$

Fig. 1 shows the redshift evolution of these distances in the adopted FLRW spacetime.

The derivatives of each distance measure in terms of the redshift are also necessary. Remembering Eqs. (15), (17) and (19) one can easily conclude that,

$$\frac{d(d_A)}{dz} = \frac{dS}{dz} \frac{dr}{dS} \frac{d(d_A)}{dr} = -\frac{S^2}{S_0} \left[r + S \left(\frac{dS}{dr} \right)^{-1} \right]. \quad (25)$$

Similarly, both $d(d_L)/dz$ and $d(d_G)/dz$ are easily obtained, whereas $d(d_z)/dz$ comes directly from Eq. (20).

Finally, the cumulative number counts N is derived as follows. The number of cosmological sources per proper volume unit n is related to the matter density ρ_m by means of,

$$n = \frac{N}{V_{Pr}} = \frac{\rho_m}{\mathcal{M}_g}, \quad (26)$$

where V_{Pr} is the proper volume. As shown by Ir12, in the FLRW cosmology the right-hand side of the Einstein equations allows

us to write the number density in terms of the proper volume as follows,

$$n = \left(\frac{3\Omega_{m_0} H_0^2 S_0^3}{8\pi G \mathcal{M}_g} \right) \frac{1}{S^3}. \quad (27)$$

In what follows we shall need to write the number density in terms of the comoving volume V_C and, therefore, a conversion between V_{Pr} and V_C is needed. In the FLRW model this is given by $V_{Pr}/V_C = S^3$, since $V_C = (4/3)\pi r^3$ and $V_{Pr} = (4/3)\pi r^3 S^3$.

3.2. Observational Quantities

The next step is to specialize the expressions above to obtain observational counterparts based on the LF data of a specific galaxy catalog. To do so we need to use the methodology advanced by RS03 connecting theoretical expressions to astronomically derived quantities.

In summary, assuming that an observational quantity $[T]_{\text{obs}}$ can be related to its theoretical counterpart T by means of a *consistency function* J such that $[T]_{\text{obs}} = JT$, then the relationship between the *selection function* ψ , which gives the volume number density of galaxies with luminosity above a given threshold, to the comoving volume number density $n_c(z)$ can be written as follows,

$$\psi(z) = J(z) n_c(z). \quad (28)$$

The redefinition of the number density in terms of comoving volume is a consequence of the fact that in observational cosmology this is the most adopted volume definition, rather than the proper volume commonly found in theoretical calculations. Hence,

$$n_c = \frac{N}{V_C} = \frac{3N}{4\pi r^3}. \quad (29)$$

What the Eq. (28) tells us is that the consistency function basically represents the undetected mass fraction in relation to the one predicted by theory. It also includes the galaxy redshift survey data, since the selection function is written in terms of the LF ϕ as follows,

$$\psi(z) = \int_{l_{\text{lim}}(z)}^{\infty} \phi(l) dl, \quad (30)$$

where $l_{\text{lim}}(z)$ is the lower luminosity threshold below which cosmological sources are not observed.

The galaxy LF is a number density per unit of luminosity, obtained by fitting the galaxy distribution in a given dataset to some function and determining its parameter values. The most common analytical form used to fit galaxy survey data is the Schechter (1976) function, given as below,

$$\phi(l) = \phi^* l^\alpha e^{-l}. \quad (31)$$

Here $l \equiv L/L_*$, L is the observed luminosity, L_* is the luminosity scale parameter, ϕ^* is a normalization parameter and α gives the faint-end slope parameter. It was found by several works that the LF evolves with the redshift (Iribarrem et al. 2012, 2013, 2014 and references therein).

The observational quantities of interest studied in this paper require previous knowledge of the observed differential number counts $[dN/dz]_{\text{obs}}$. Therefore, linking this quantity to its theoretical counterpart is an essential step, yielding (Ir12),

$$\left[\frac{dN}{dz} \right]_{\text{obs}} = J(z) \frac{dN}{dz} = \frac{\psi(z)}{n_c(z)} \frac{dN}{dz}. \quad (32)$$

This is our key equation relating the relativistic theory to the observations. Thus, the observed cumulative number counts can be calculated as,

$$[N(z)]_{\text{obs}} = \int_0^z \left[\frac{dN}{dz'} \right]_{\text{obs}} dz', \quad (33)$$

and, as discussed in Ir12, the uncertainty in $[N]_{\text{obs}}$ can be estimated from the uncertainty in $[dN/dz]_{\text{obs}}$.

Note that the approach summarized above indicates that all observational quantities obtained by applying $J(z)$ to their theoretical counterparts will inherit the same empirical number count redshift evolution encoded in the parametrization of the LF. In addition, Eq. (28) shows that the consistency function is independent of volume units and, hence, if an observational quantity is obtained using $J(z)$ its original volume unit dependence is preserved.

3.3. FORS Deep Field Galaxy Redshift Survey

As seen above, the consistency function is required for the calculation of the observational quantities, but to do so one needs first to compute the selection function in terms of the redshift in a given galaxy redshift survey. That was done by Ir12, where one can find a very thorough discussion of the procedure adopted in the calculation of the FDF selection functions, as well as details of the numerical scheme. Hence, what we shall present below is a summary of Ir12's methodology on this respect.

G04 and G06 fitted the LF Schechter parameters over the redshifts of 5558 I-band selected galaxies in the FORS Deep Field dataset, photometrically measured down to an apparent magnitude limit of $I_{AB} = 26.8$. All galaxies were selected in the I-band and then had their magnitudes for each of the five blue bands (1500 Å, 2800 Å, u' , g' and B) and the three red ones (r' , i' and z') computed using the best fitting SED given by the photometric redshift code developed by the authors convolved with the associated filter function. G04 and G06 determined the photometric redshifts by fitting template spectra to the measured fluxes on the optical and near infrared images of the galaxies. The redshift ranges of $0.75 \leq z \leq 3.0$ for the red bands and $0.5 \leq z \leq 5.0$ for the blue bands.

To calculate the actual values of the selection functions at each waveband, we need the result obtained in RS03 for the limited bandwidth version of the selection function of a given LF, fitted by a Schechter's analytical profile (Eqs. 30 and 31). In terms of the absolute magnitudes $M(z)$ this expression reads,

$$\psi^W(z) = 0.4 \ln 10 \int_{-\infty}^{M_{\text{lim}}^W(z)} \phi^*(z) 10^{0.4[1+\alpha(z)][M^*(z)-\bar{M}^W]} \times \exp\{-10^{0.4[M^*(z)-\bar{M}^W]}\} d\bar{M}^W, \quad (34)$$

where the index W indicates the bandwidth filter. The expressions for the redshift evolution of the LF parameters adopted by G04 and G06 are,

$$\begin{aligned} \phi^*(z) &= \phi_0^* (1+z)^{B^W}, \\ M^*(z) &= M_0^* + A^W \ln(1+z), \\ \alpha(z) &= \alpha_0, \end{aligned}$$

where A^W and B^W are the evolution parameters fitted for the different W bands and M_0^* , ϕ_0^* and α_0 the local ($z \approx 0$) values of the Schechter parameters. Since all galaxies were detected and selected in the I-band, we can write,

$$M_{\text{lim}}^W(z) = M_{\text{lim}}^I(z) = I_{\text{lim}} - 5 \log[d_L(z)] - 25 + A^I, \quad (35)$$

for a luminosity distance d_L given in Mpc. $I_{\text{lim}} = 26.8$ is the limiting apparent magnitude of the I-band in the FDF survey. Its reddening correction is $A^I = 0.035$ (Heidt et al. 2001).

The selection functions for all eight bands of the dataset were calculated by Ir12 using simple numerical integrations at equally spaced values spanning the whole redshift interval. The UV bands, 1500 Å, 2800 Å, and u' , evolve tightly with redshift, having values that are consistent with each other within the uncertainties, while assuming values outside the uncertainties of the ones calculated in the blue optical bands g' , and B . Due to this, Ir12 chose to use the selection functions of the combined UV bands and those of the combined blue optical bands separately. The selection functions in the red-band dataset of G06, r' , i' and z' were also combined. Once the combined selection functions were obtained, Ir12 calculated $[dN/dz]_{\text{obs}}$ by means of Eq. (32).

4. Power Spectrum Analysis of the FDF Survey

The observational values of the differential number counts $[dN/dz]_{\text{obs}}$ for all filters in the dataset allowed us to evaluate the observational differential number densities $[\gamma]_{\text{obs}}$ for the FLRW cosmology distance measures discussed above by simply replacing dN/dz with $[dN/dz]_{\text{obs}}$ in Eq. (4). The dependence of these densities on the distance definitions are shown in Fig. 2. Similarly, the observational values of the integral densities $[\gamma^*]_{\text{obs}}$ were obtained by replacing N with $[N]_{\text{obs}}$ in Eq. (5). The results are shown in Fig. 3.

The differential density constructed with the area distance d_A becomes discontinuous at $z \approx 1.6$ because d_A reaches a maximum at that redshift and, therefore, its derivative with respect to z vanishes, rendering $[\gamma_A]_{\text{obs}}$ undefined. In addition, due to this maximum $[\gamma_A^*]_{\text{obs}}$ has a curious turn around in d_A at $z \approx 1.6$, as shown in Fig. 3. Nevertheless, Fig. 4 shows that such a curious behavior does not occur when the integral density γ_A^* is plotted in terms of z , which in this case keeps on increasing. This is due to the fact that each d_A corresponds to two redshift values (see Fig. 1), but since each z produces only one γ_A^* , each d_A generates then two values for z and γ_A^* . The single point where this behavior is absent is when d_A reaches its maximum, which corresponds to single values for d_A , z and γ_A^* . This effect is better visualized in Fig. 5 where a redshift scale was added to the right side of each plot. One should point out that the singular point where d_A reaches a maximum plays an unique geometrical role and has an associated mass which can be calculated by means of few assumptions on the cosmological model, providing them a measurable cosmological characteristic (Hellaby 2006).

Fig. 6 shows the PS of the FDF observational differential densities $P_k[\gamma_i]_{\text{obs}}$ and their theoretical counterparts plotted against the wave number k_i and the redshift. The observational points were determined by means of the combined UV, optical and red bands in the G04 and G06 dataset. It is clear from the graphs that $P_k[\gamma_A]_{\text{obs}}$ possesses an odd behavior due to its discontinuity at $z \approx 1.6$, bearing no resemblance to the PS of the two-point correlation function, whereas the other power spectra $P_k[\gamma_{i=G,L,Z}]_{\text{obs}}$ show a similar behavior to the two-point correlation function PS as presented by Tegmark et al. (2004, Fig. 38). We note that these authors calculated the two-point correlation function PS using different types of data, such as cosmic background radiation, galaxies, clusters of galaxies, lensing and Lyman alpha forest. Nevertheless, their general PS behavior is basically similar to ours, apart from the one calculated with d_A .

The PS of the observational integral densities in the UV, optical and red combined bands versus the wave number and the

redshift are shown in Fig. 7. We note that $P_k[\gamma_{i=G,L,Z}^*]_{\text{obs}}$ differ from $P_k[\gamma_{i=G,L,Z}]_{\text{obs}}$ shown in the previous figure only at small wave number values or, equivalently, at higher redshifts. Such difference occurs because the differential densities measure the rate of growth in number counts since $\gamma_i \propto dN/dz$, whereas $\gamma_i^* \propto N$ (see Eqs. 4 and 5). As N is a cumulative quantity, it can only increase or remain constant, while dN/dz increases, reaches a maximum and then decreases at scales dependent on the ratio of increase in N . Clearly the declining behavior of dN/dz will occur at higher values of z , beyond its maximum, leading the decline in γ to become even more pronounced at those scales. In addition, by measuring the rate of growth in number counts, γ is more sensitive to local fluctuations due to noisy data. Thus, the steeper decline detected in the slopes of $P_k[\gamma_{i=G,L,Z}]_{\text{obs}}$ at small wave numbers as compared to those at $P_k[\gamma_{i=G,L,Z}^*]_{\text{obs}}$ can be attributed to these distortion effects at the redshift limits of the sample.

As discussed above, the radial correlation $\Xi_i(d_i)$ was studied by Ribeiro (1995) in the Einstein-de Sitter (EdS) model, but only with the luminosity distance. Here we extend the analysis of Eq. (7) to the galaxy area distance and redshift distance in the FLRW model with $\Omega_m = 0.3$ and $\Omega_\Lambda = 0.7$. These results are shown in Fig. 8 where one can see that, similarly to the EdS cosmology, the amplitude of $[\Xi_L]_{\text{obs}}$ in the FLRW model also depends on the sample size. The extension of these results to d_z and d_G are presented in Fig. 9, where different sample sizes were used, confirming thus such a dependence. Due to the pathological behavior of d_A , $[\Xi_A]_{\text{obs}}$ was not evaluated.

Once in possession of the $[\Xi_{i=G,L,Z}]_{\text{obs}}$ computations for the FDF dataset, it is natural to look at the behavior of their respective power spectrum. Fig. 10 shows such PS results, where one can see a distortion at small wave numbers probably caused by the subtraction of one in Eq. (7). To see if that is actually the reason behind this distortion, we evaluated the PS of the ratio γ/γ^* for d_L , d_z and d_G . Graphs of these quantities are shown in Fig. 11 where we can clearly see the absence of the previous distortion. Finally, the PS of the ratio γ/γ^* for the area distance are shown in Fig. 12 where the discontinuity in γ_A and $[\gamma_A]_{\text{obs}}$ translates themselves to discontinuous behavior for $P_k[\gamma_A/\gamma_A^*]_{\text{obs}}$.

5. Conclusion

In this paper we have studied the theoretical and observational power spectrum of the differential and integral galaxy volume number densities γ and γ^* using various relativistic cosmology distance measures d_i , namely the angular diameter distance d_A , galaxy area distance d_G , luminosity distance d_L and redshift distance d_z ($i = A, G, L, Z$). The cosmology adopted here is the FLRW model with non zero cosmological constant Λ having $\Omega_{m_0} = 0.3$, $\Omega_{\Lambda_0} = 0.7$ and $H_0 = 70 \text{ km s}^{-1} \text{ Mpc}^{-1}$. Observational results were obtained by following the framework that connects the relativistic cosmology number counts theory with the astronomical data extracted from the galaxy luminosity function (LF), as proposed by Ribeiro & Stoeger (2003) and further developed by Albani et al. (2007) and Iribarrem et al. (2012). This framework uses the LF parameters of the FDF galaxy survey provided by Gabasch et al. (2004, 2006) in order to calculate the observed differential number counts $[dN/dz]_{\text{obs}}$ required to build the observational densities $[\gamma_i]_{\text{obs}}$ and $[\gamma_i^*]_{\text{obs}}$. The observational results were produced in the combined red, blue optical and UV bands in the redshift range $0.5 \leq z \leq 5.0$.

The PS of the galaxy volume number densities were obtained directly from both $[\gamma_i]_{\text{obs}}$ and $[\gamma_i^*]_{\text{obs}}$ and two other combinations

of these quantities, namely the ratio $[\gamma_i/\gamma_i^*]_{\text{obs}}$ and the radial correlation $[\Xi_i]_{\text{obs}}$ which mixes up these two densities in a way that they can be discussed in terms of the sample size and each distance measure used above. Therefore, our analysis was able to compute $P_k[\gamma_i]_{\text{obs}}$, $P_k[\gamma_i^*]_{\text{obs}}$, $P_k[\gamma_i/\gamma_i^*]_{\text{obs}}$ and $P_k[\Xi_i]_{\text{obs}}$.

The results show that the graphs for $P_k[\gamma_{i=G,L,Z}]_{\text{obs}}$, $P_k[\gamma_{i=G,L,Z}^*]_{\text{obs}}$ and $P_k[(\gamma_i/\gamma_i^*)_{i=G,L,Z}]_{\text{obs}}$ have similar behavior for larger wave numbers, but the first differs from the other two at small wave numbers. Both $P_k[\gamma_{i=G,L,Z}^*]_{\text{obs}}$ and $P_k[(\gamma_i/\gamma_i^*)_{i=G,L,Z}]_{\text{obs}}$ have general power-law behavior, whereas $P_k[\gamma_{i=G,L,Z}]_{\text{obs}}$ behaves more similarly to the PS derived from the 2-point correlation function (see Fig. 38 of Tegmark et al. 2004) having a more pronounced decline at very small wave numbers.

The PS analysis using d_A is problematic because this distance measure starts increasing, reaches a maximum and then decreases, resulting in a discontinuous $[\gamma_A]_{\text{obs}}$ at $z \approx 1.6$. Therefore, both $P_k[\gamma_A]_{\text{obs}}$ and $P_k[\gamma_A/\gamma_A^*]_{\text{obs}}$ also present discontinuities. $P_k[\gamma_A^*]_{\text{obs}}$ is, however, continuous, but has a minimum wave number value just as d_A has a maximum.

The radial correlation Ξ_i , a quantity defined to possibly exhibit sample dependence in observational values, actually showed such a dependence for $[\Xi_{i=G,L,Z}]_{\text{obs}}$, confirming a previous theoretical prediction made by using only the luminosity distance d_L (Ribeiro 1995). Nevertheless, their respective PS $P_k[\Xi_{i=G,L,Z}]_{\text{obs}}$ present some strong distortions.

In summary, the study presented here suggests that the PS analysis of the galaxy volume number densities can be considered as a complementary tool for studies of the large-scale galaxy distribution. That may be particularly the case of models describing the galaxy distribution as a fractal system, as advanced by Conde-Saavedra et al. (2015) and Teles et al. (2021).

Acknowledgements. We thank Filipe B. Abdalla for the original suggestion which motivated this paper. A.R.L. and M.B.R. are respectively grateful to CAPES and FAPERJ for the financial support.

References

- Albani, V.V.L., Iribarrem, A.S., Ribeiro, M.B., and Stoeger, W.R. 2007, *ApJ*, 657, 760-772, arXiv:astro-ph/0611032 (**A07**)
- Conde-Saavedra, G., Iribarrem, A., Ribeiro, M.B. 2015, *Physica A*, 417, 332-344, arXiv:1409.5409
- Ellis, G.F.R. 1971, in *General Relativity and Cosmology*, ed. R.K. Sachs (Proc. Int. School Phys. "Enrico Fermi"; New York: Academic Press); reprinted in *Gen. Rel. Grav.*, 41, 581, 2009
- Ellis, G.F.R. 2007, *Gen. Rel. Grav.*, 39, 1047-1052
- Etherington, I.M.H. 1933, *Phil. Mag. ser. 7*, 15, 761; reprinted in *Gen. Rel. Grav.*, 39, 1055, 2007
- Gabasch, A. et al. 2004, *A&A*, 421, 41-58 (**G04**)
- Gabasch, A. et al. 2006, *A&A*, 448, 101 (**G06**)
- Gabrielli, A. et al. 2005, *Statistical Physics for Cosmic Structures* (Springer Verlag)
- Heidt, J. et al. 2001, *The FORS Deep Field*, *Reviews in Modern Astronomy*, Vol. 14, R.E. Schielicke (Ed.), *Astronomische Gesellschaft*
- Hellaby, C. 2006, *MNRAS*, 370, 239
- Holanda, R.F.L., Lima, J.A.S., and Ribeiro, M.B. 2010, *ApJ*, 722, L233, arXiv:1005.4458
- Holanda, R.F.L., Lima, J.A.S., and Ribeiro, M.B. 2011, *A&A*, 528, L14, arXiv:1003.5906
- Holanda, R.F.L., Lima, J.A.S., and Ribeiro, M.B. 2012, *A&A*, 538, A131, arXiv:1104.3753
- Iribarrem, A.S., Lopes, A.R., Ribeiro, M.B., and Stoeger, W.R. 2012, *A&A*, 539, A112, arXiv:1201.5571, (**Ir12**)
- Iribarrem, A. et al. 2013, *A&A*, 558, A15, arXiv:1308.2199
- Iribarrem, A. et al. 2014, *A&A*, 563, A20, arXiv:1401.6572
- Lin, H. et al. 1999, *ApJ*, 518, 533-561
- Martínez, V.J., and Saar, E. 2002, *Statistics of the Galaxy Distribution* (Chapman & Hall/CRC)
- Pietronero, L. 1987, *Physica A*, 144, 257

- Plebański, J., and Krasinski, A. 2006, *An Introduction to General Relativity and Cosmology* (Cambridge University Press)
- Rangel Lemos, L.J., and Ribeiro, M.B. 2008, *A&A*, 488, 55-66, arXiv:0805.3336
- Ribeiro, M.B. 1995, *ApJ*, 441, 477-487, arXiv:astro-ph/9910145
- Ribeiro, M.B. 2001, *Gen. Rel. Grav.*, 33, 1699-1730, arXiv:astro-ph/0104181
- Ribeiro, M.B. 2005, *A&A*, 429, 65-74, arXiv:astro-ph/0408316
- Ribeiro, M.B., and Stoeger, W.R. 2003, *ApJ*, 592, 1-16, arXiv:astro-ph/0304094
(RS03)
- Schechter, P. 1976, *ApJ*, 203, 297-306
- Sparke, L.S., and Gallagher, J.S. 2000, *Galaxies in the Universe* (Cambridge University Press)
- Sylos Labini, F. et al. 1998, *Phys. Rep.*, 293, 61-226
- Tegmark, M. et al. 2004, *ApJ*, 606, 702-740
- Tegmark, M. et al. 2006, *Phys. Rev. D*, 74, 123507
- Teles, S., Lopes, A.R., Ribeiro, M.B. 2021, *Phys. Lett. B*, 813, 136034, arXiv:2012.07164

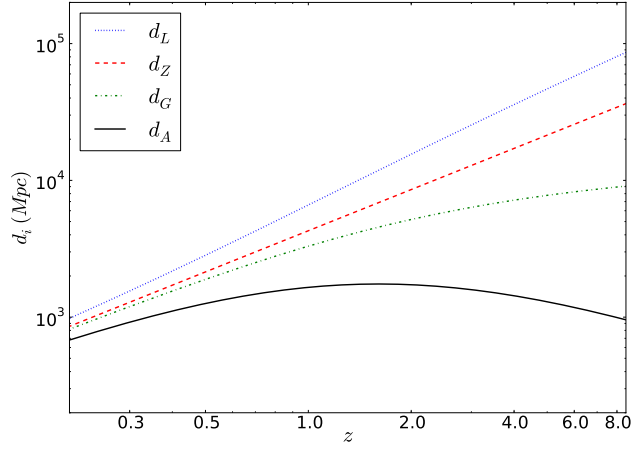


Fig. 1. Redshift evolution of the four FLRW cosmological distance measures adopted here assuming $\Omega_m = 0.3$, $\Omega_\Lambda = 0.7$ and $H_0 = 70 \text{ km s}^{-1} \text{ Mpc}^{-1}$. Symbols are as in the legend.

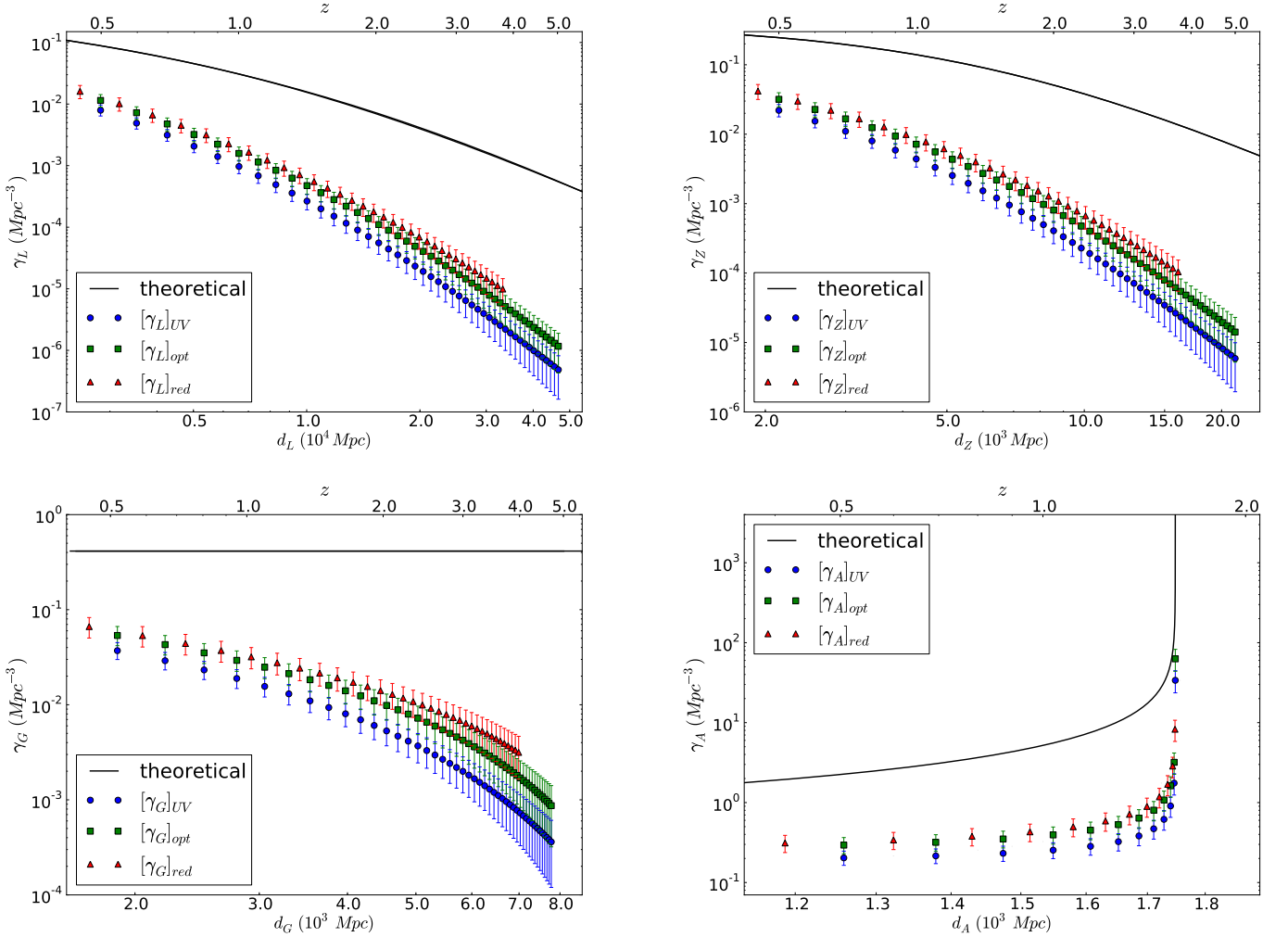


Fig. 2. These plots show the theoretical and observational relativistic differential densities for the four FLRW cosmological distances adopted here. The observational densities are shown in the combined UV, optical and red bands of the FDF datasets of G04 and G06. Symbols are as in the legend.

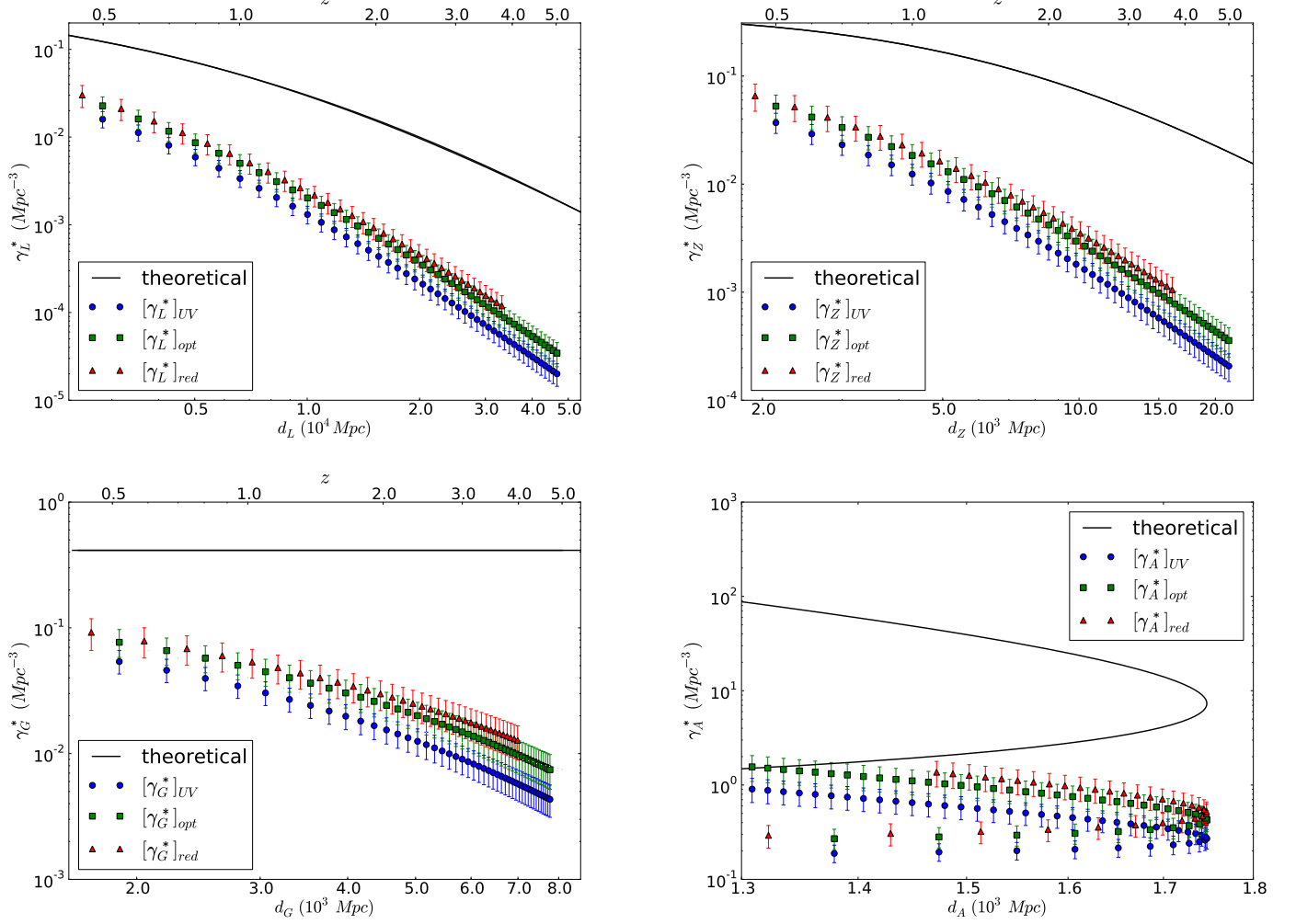


Fig. 3. Plots showing the theoretical and observational relativistic integral densities for the four FLRW cosmological distances adopted here. The observational points are shown in the combined UV, optical and red bands of the FDF datasets of G04 and G06. Symbols are as in the legend.

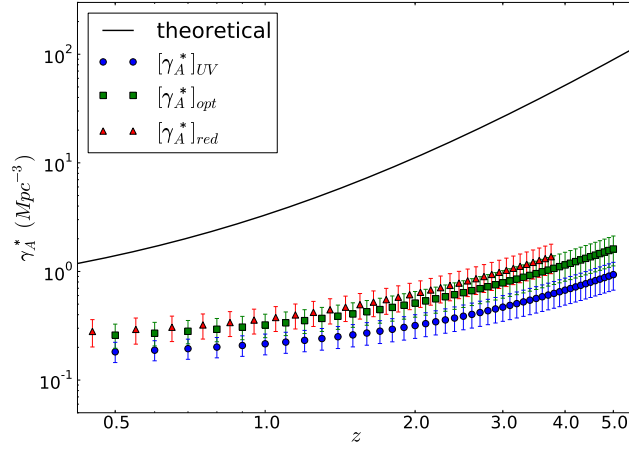


Fig. 4. This graph shows the theoretical and observational relativistic integral densities obtained with the angular diameter distance d_A against the redshift. The observational points are in the combined UV, optical and red bands of the FDF datasets of G04 and G06. Note the difference between this plot (γ_A^* vs. z) and the one in the lower right panel of Fig. 3 (γ_A^* vs. d_A), although the Y-axis scale is basically the same. Symbols are as in the legend.

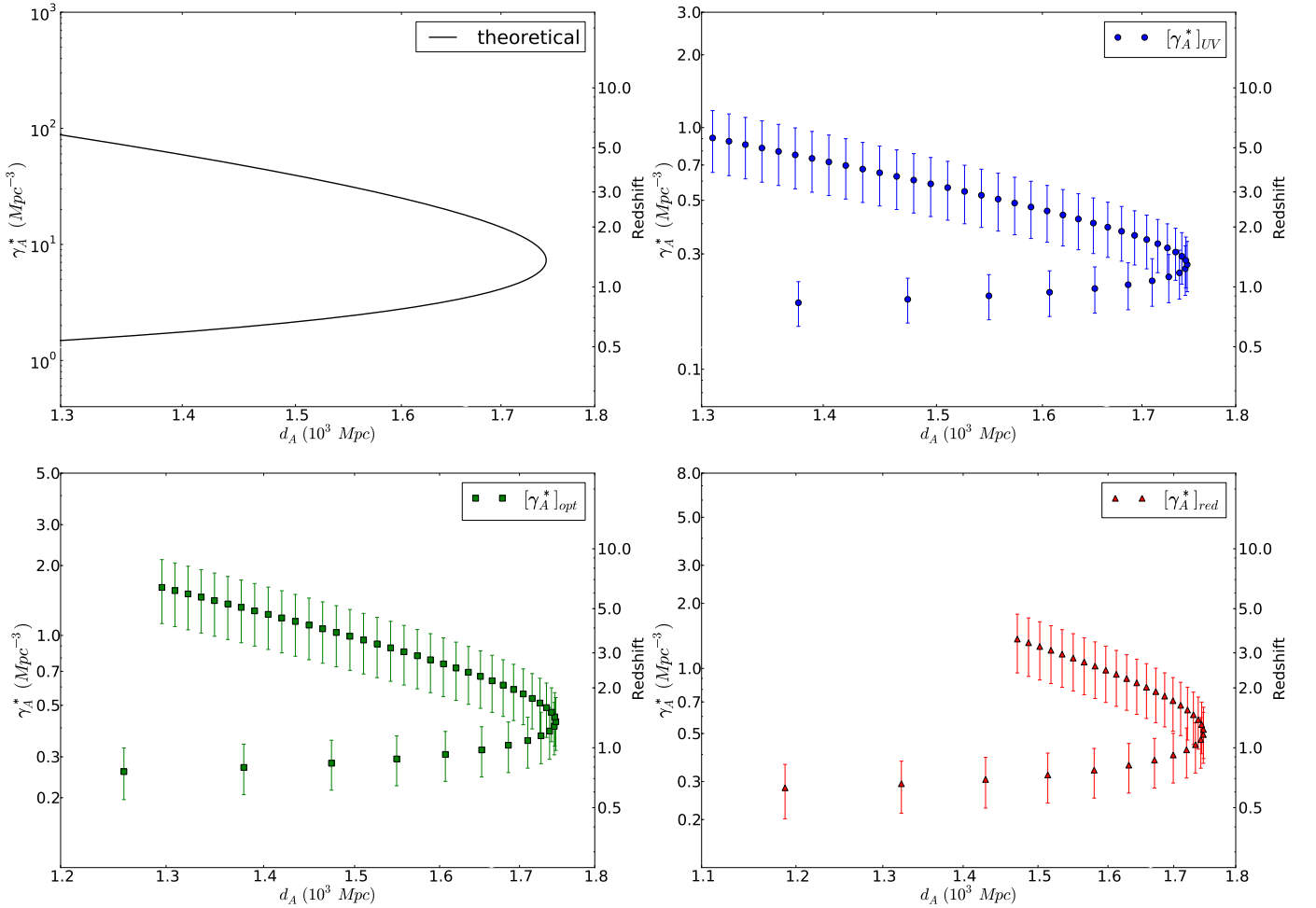


Fig. 5. This figure shows the theoretical and observational relativistic integral densities computed with the angular diameter distance versus d_A and the redshift. These graphs combine the information of Figs. 1 and 4, basically splitting the lower right plot of Fig. 3 in four different plots and adding a redshift scale at the right side of each graph. Note that for the same redshift scale on the right side of each plot one needs a different scale for γ_A^* on the left side.

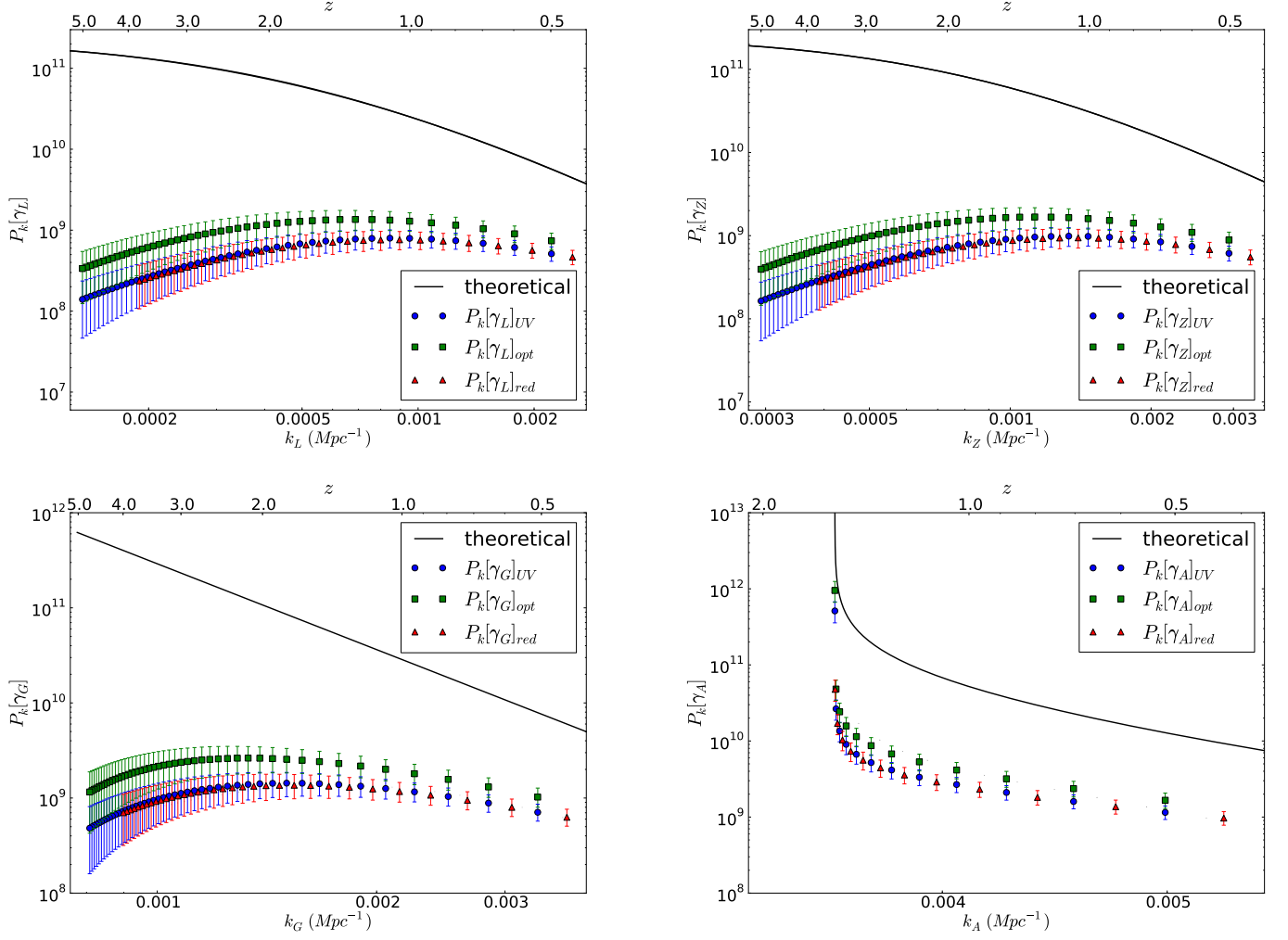


Fig. 6. This figure shows a panel with the power spectra of the theoretical and observational relativistic differential densities computed with the four FLRW cosmological distances adopted here. The observational points are presented in the combined UV, optical and red bands of the FDF datasets of G04 and G06. Symbols are as in the legend.

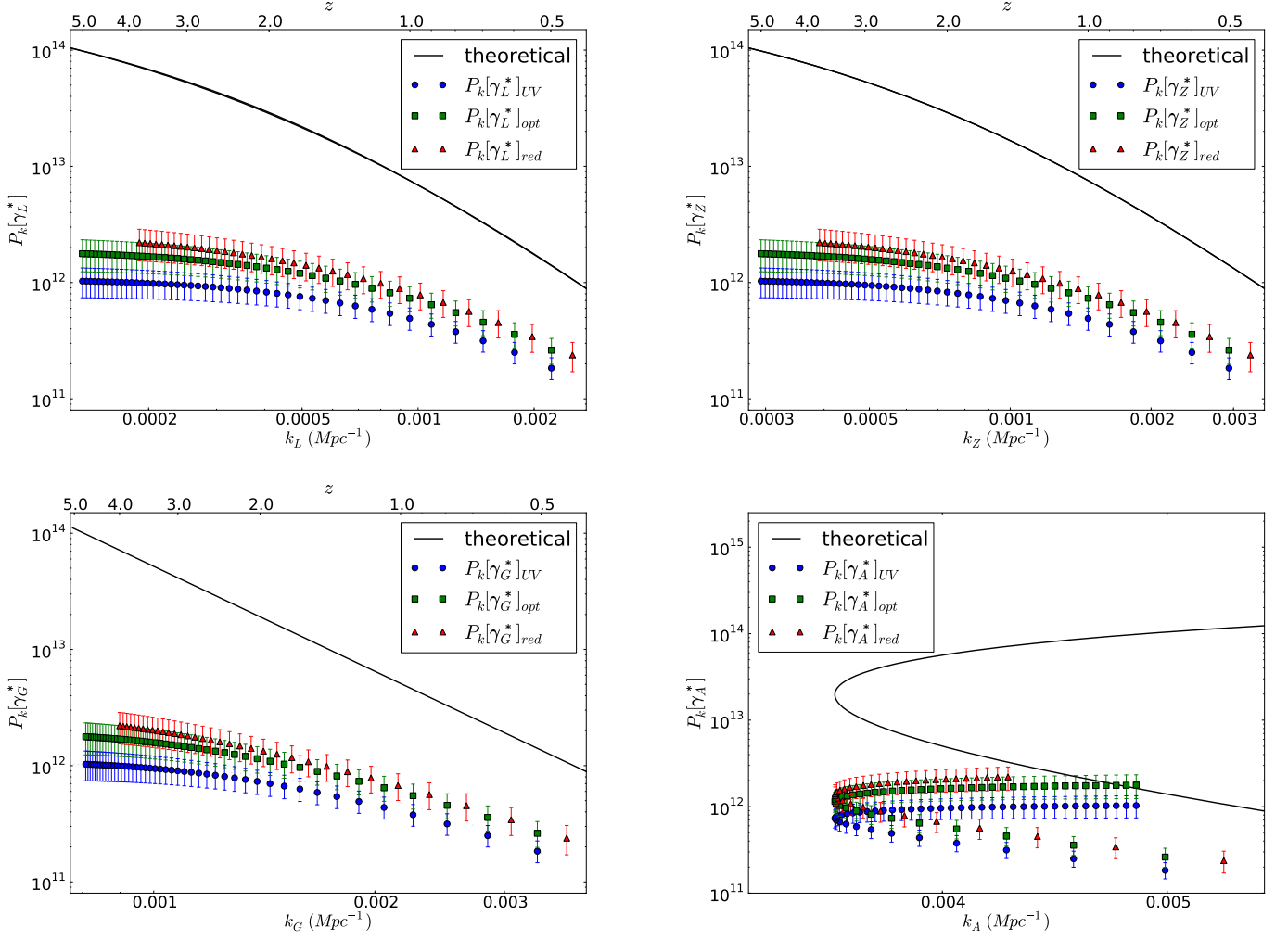


Fig. 7. Panel showing the power spectrum of theoretical and observational relativistic integral densities. The observational points are presented in the combined UV, optical and red bands of the FDF datasets of G04 and G06. Symbols are as in the legend.

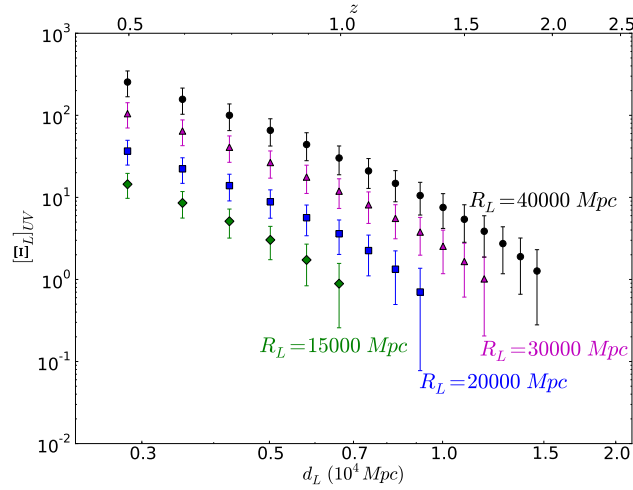


Fig. 8. Graph of the radial correlation for the luminosity distance in the combined UV waveband for different sample sizes. Symbols are as in the legend.

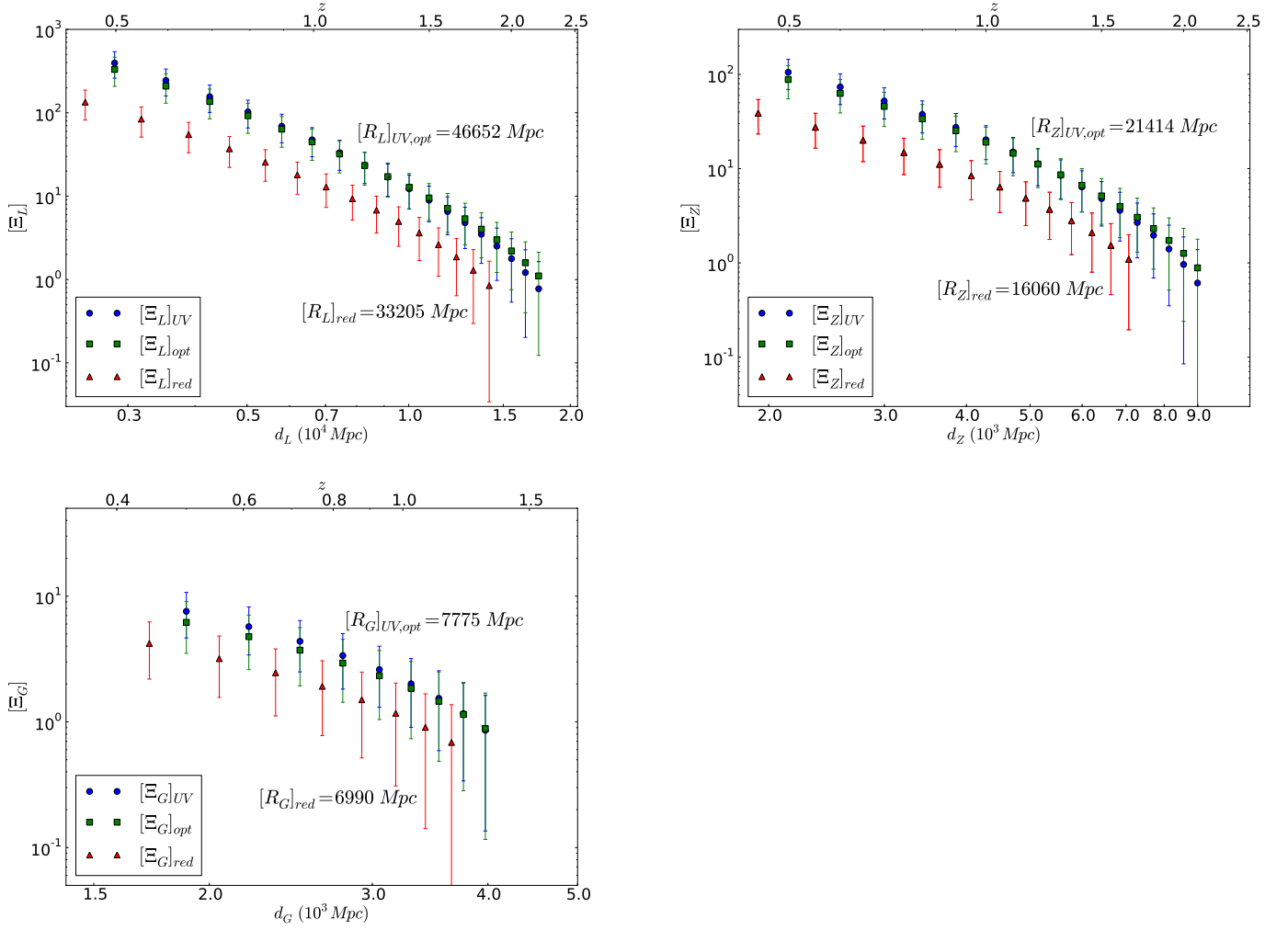


Fig. 9. Radial correlation for the luminosity distance, redshift distance and galaxy area distance in the combined UV, optical and red bands of the FDF datasets of G04 and G06. Symbols are as in the legend.

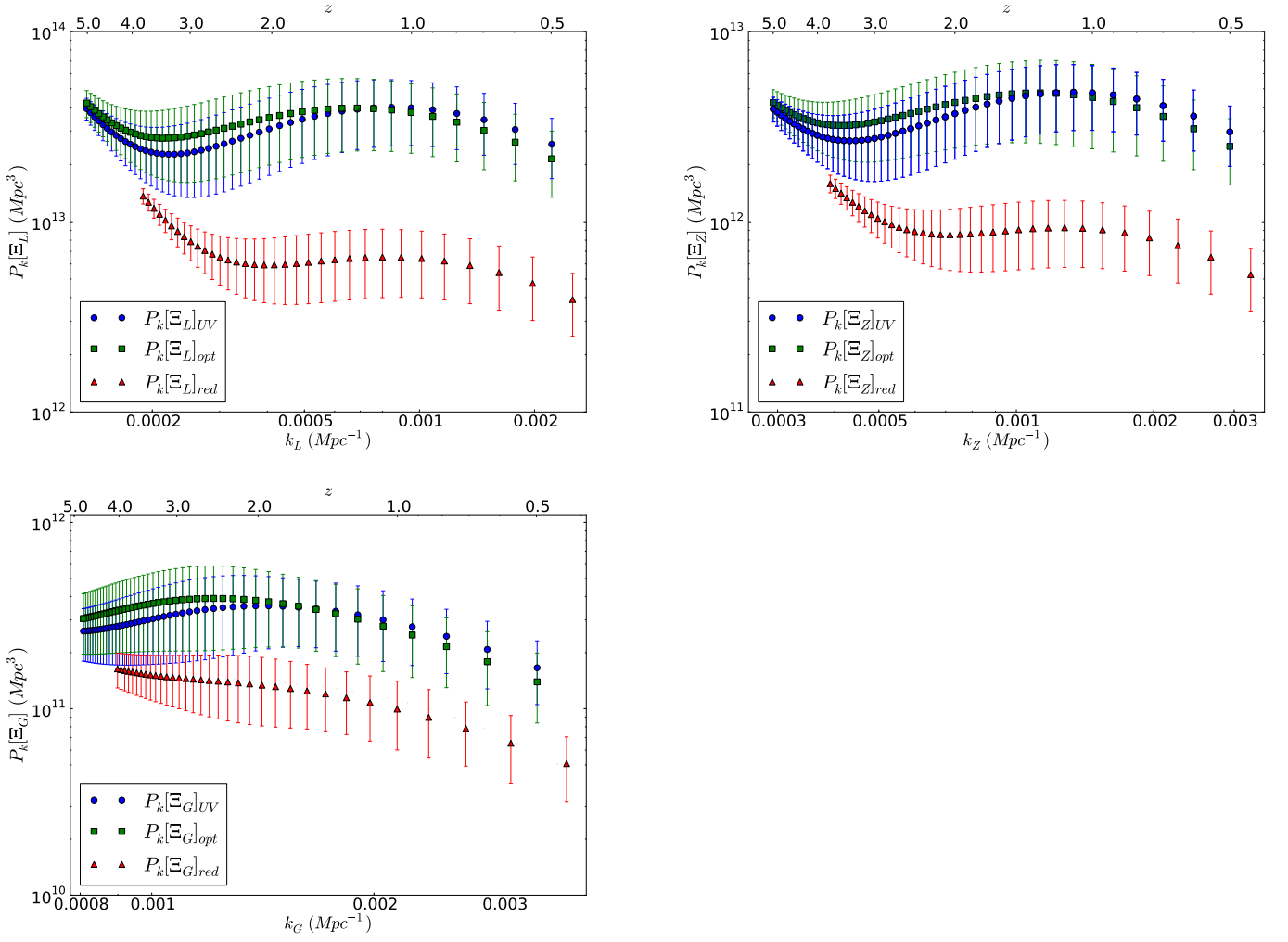


Fig. 10. PS of Radial correlation for the luminosity distance, redshift distance and galaxy area distance in the combined UV, optical and red bands of the FDF datasets of G04 and G06. Symbols are as in the legend.

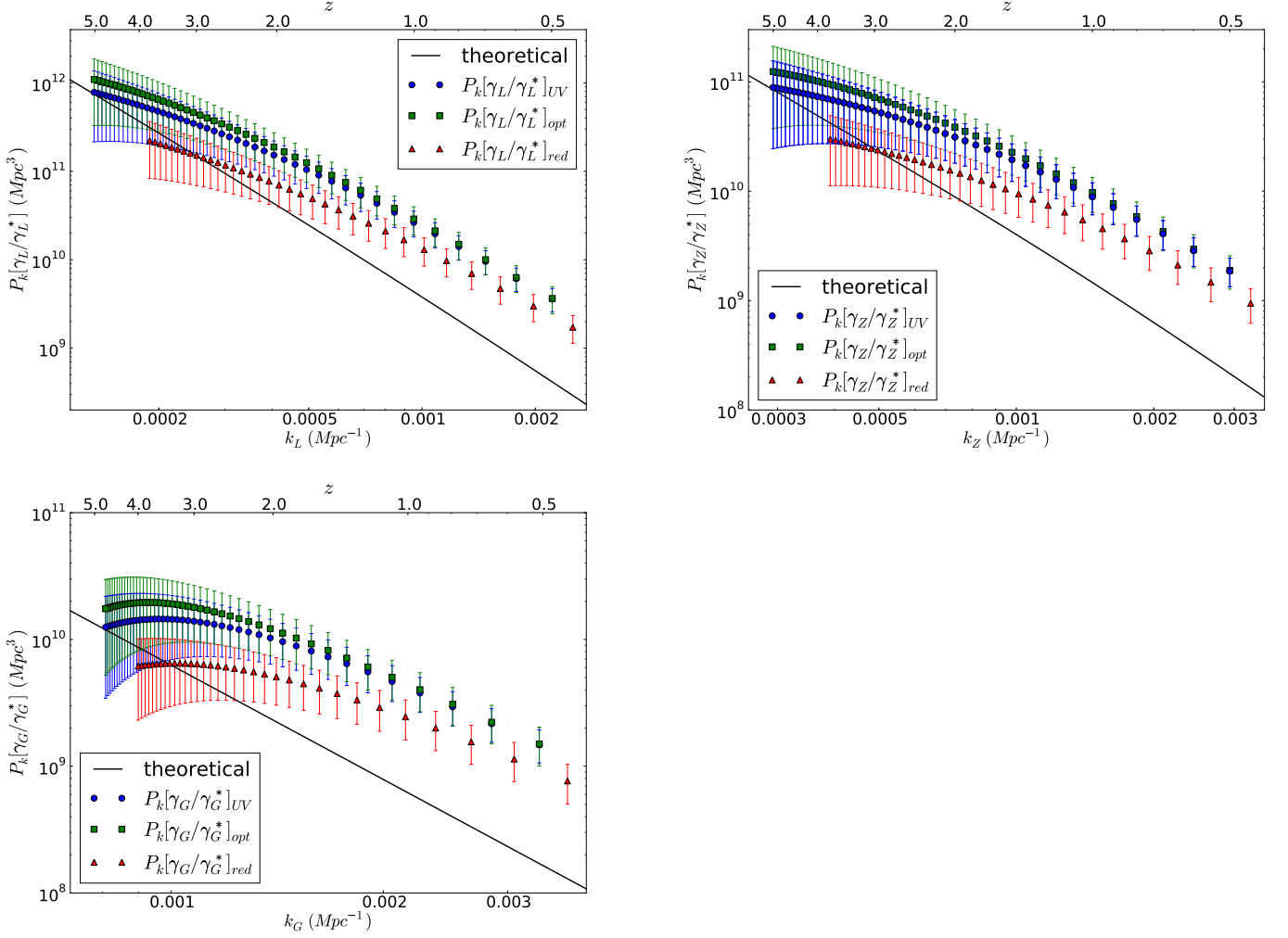


Fig. 11. PS of the ratio γ/γ^* for the luminosity distance, redshift distance and galaxy area distance in the combined UV, optical and red bands of the FDF datasets of G04 and G06. Symbols are as in the legend.

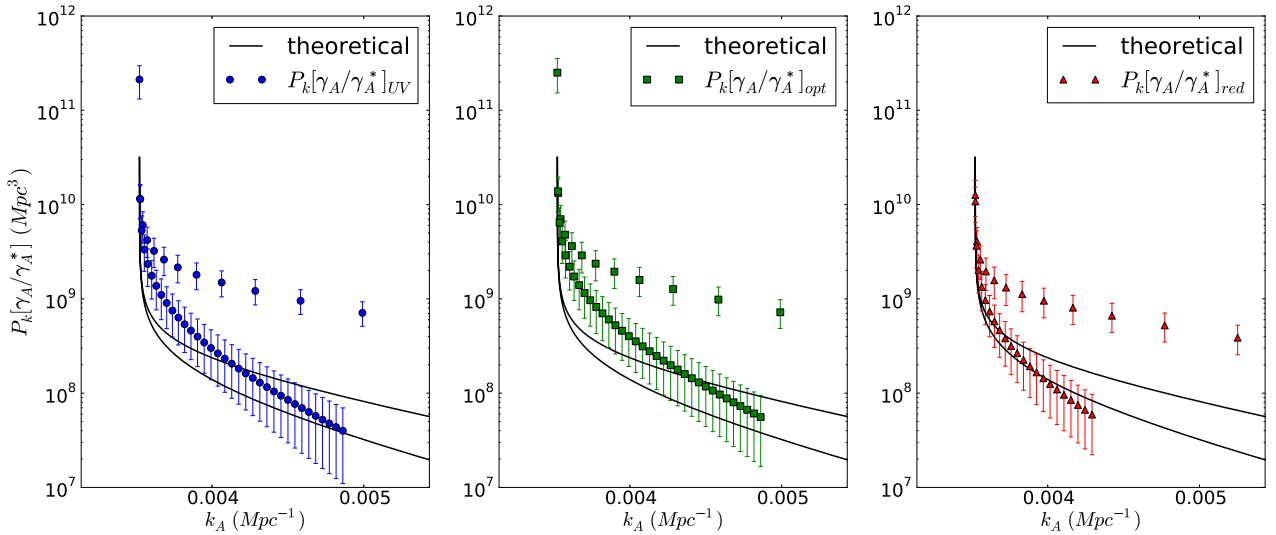


Fig. 12. PS of the ratio γ/γ^* for the area distance in the combined UV, optical and red bands of the FDF datasets of G04 and G06. Symbols are as in the legend.

